

ISOSCELES: Grid of stellar atmosphere and hydrodynamic models of massive stars. The first results

Ignacio Araya¹, Michel Curé², Natalia Machuca² and Catalina Arcos²

¹Vicerrectoría de Investigación, Universidad Mayor, Chile

²Instituto de Física y Astronomía, Universidad de Valparaíso, Chile

Abstract. In this work we seek to derive simultaneously the stellar and wind parameters of massive stars, mainly A and B type supergiant stars. Our stellar properties encompass the effective temperature, the surface gravity, the micro-turbulence velocity and, silicon abundance. For wind properties we consider the line-force parameters (α , k and δ) obtained from the standard line-driven wind theory. To model the data we use the radiative transport code FASTWIND considering the hydrodynamic solutions derived with the stationary code HYDWIND. Then, ISOSCELES, a grid of stellar atmosphere and hydrodynamic models of massive stars is created. Together with the observed spectra and a semi-automatic tool the physical properties from these stars are determined through spectral line fittings. This quantitative spectroscopic analysis provide an estimation about the line-force parameters. In addition, we confirm that the hydrodynamic solutions, called δ -slow solutions, describe quite reliable the radiation line-driven winds of B supergiant stars.

Keywords. stars: early-type, stars: mass loss, stars: winds, outflows, hydrodynamics, techniques: spectroscopic

1. Introduction

ISOSCELES, GrId of Stellar AtmOSphere and HydrodynamIc ModelS for MassivE Stars, is the first grid of synthetic data for massive stars that involves both, the m-CAK hydrodynamics (instead of the generally used β -law) and the NLTE radiative transport.

ISOSCELES covers the complete parameter space of O-, B- and A-type stars. To produce the grid of synthetic line profiles, we first computed a grid of hydrodynamic wind solutions with our stationary code HYDWIND (Curé 2004). These hydrodynamic wind solutions, based on the CAK theory and its improvements (Castor et al. 1975; Friend & Abbott 1986; Curé 2004; Curé et al. 2011) are used as input in the NLTE radiative transport code FASTWIND (Puls et al. 2005).

In addition, these calculations consider the hydrodynamic solution δ -slow. This type of solution is obtained when the value of the ionization-related parameter δ takes higher values ($\delta \gtrsim 0.3$) than the ones provided by the standard m-CAK solution (Curé et al. 2011). Although these high values of δ are not calculated self-consistently (Gormaz-Matamala et al. 2019), values around 0.3 are similar to the value ($\delta = 1/3$) obtained by Puls et al. (2000) for a wind with neutral hydrogen as a trace element.

Each HYDWIND model is described by six parameters: T_{eff} , $\log g$, R_* , α , k , and δ . All these models consider, for the optical depth, the boundary condition $\tau = 2/3$, at the stellar surface. Figure 1 shows the location of the different synthetic models in the

Table 1. Range of values considered in HYDWIND and FASTWIND grids.

T_{eff} :	9 000 to 45 000 [K]
$\log g$:	0.6 to 4.5 [dex]
α :	0.45, 0.47, 0.51, 0.53, 0.55, 0.57, 0.61, 0.65
k :	0.05 to 0.60 (step size 0.05)
δ :	0.00, 0.04, 0.10, 0.14, 0.2, 0.24, 0.3, 0.31, 0.32, 0.33, 0.34, 0.35
$\log \epsilon_{\text{Si}}$:	7.21, 7.36, 7.51, 7.66, 7.81
v_{micro} :	1.0, 5.0, 10.0, 15.0, 20.0, 25.0 [km/s]

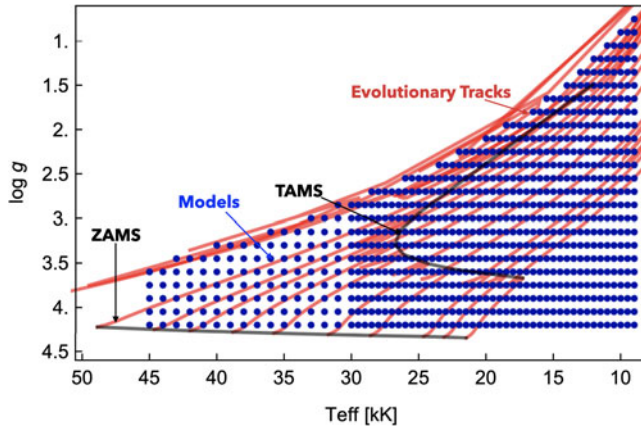


Figure 1. Location of $(T_{\text{eff}} - \log g)$ pairs (dots) considered in the grid of models. The red lines represent the evolutionary tracks from $7 M_{\odot}$ to $60 M_{\odot}$ without rotation (Ekström et al. 2008), while the black lines correspond to the zero age main-sequence (ZAMS) and the terminal age main-sequence (TAMS).

$T_{\text{eff}} - \log g$ plane. The range for the values considered in HYDWIND and FASTWIND grids are listed in Table 1. It is worth noting that not all combinations of these parameters converge to a physical stationary hydrodynamic solution. In addition, the values of δ are necessary to obtain both fast and δ -slow solutions.

In the case of the FASTWIND grid, we calculated a total of 573 433 models. From these models, line profiles of H, He, and Si elements were calculated in the optical and infrared range. Also, it is important to notice, that all our models are calculated without stellar rotation.

2. Method

We develop a methodology (script in Python) to carry out a semi-automatic analysis of an observed spectrum. The observational data was pre-processed using the *IACOB-broad* tool (Simón-Díaz & Herrero 2014) to derive the projected rotational and macroturbulent speeds. Then, these values were used in our search code to perform the spectral fitting with the purpose to obtain stellar and wind parameters. Figure 2 shows the structure of the search code.

First, the code reads an input file that contains the information of the observational data, the convolution parameters and (optional) the type of solution we are searching for, fast or δ -slow. In a second step, it uses multiprocessing tools to search through the grid. The line profiles are rotationally convolved and interpolated with the observed line. Then a χ^2 test is performed. Finally, the code collect all these results and sort them from lower to higher χ^2 values, selecting and returning the one that most resembles to the observational data.

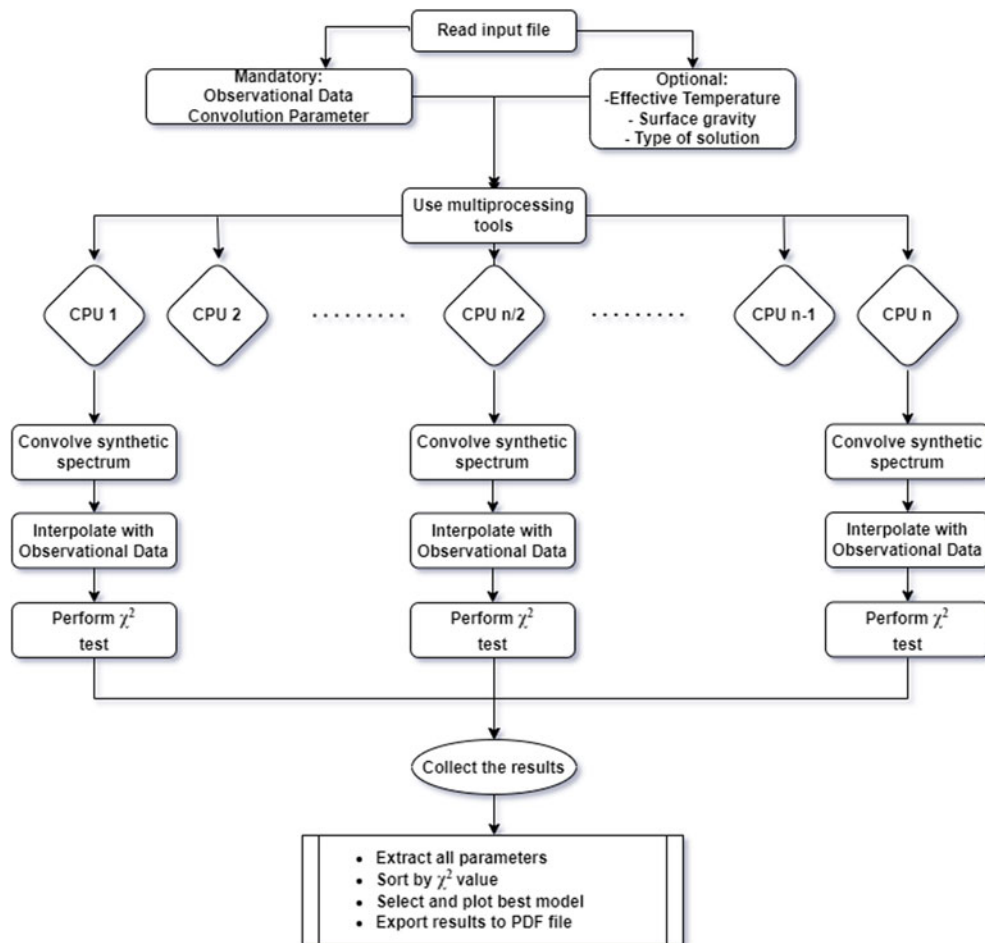


Figure 2. Diagram with our methodology to derive the stellar and wind parameters from observations.

3. First Results

By way of example, we present the results for the star HD 99953 considering six line profiles (see Figure 3). We derived stellar parameters similar to the ones obtained by Haucke *et al.* (2018). Regarding to the wind parameters, they found $\dot{M} = 0.13 \times 10^{-6} M_{\odot}/\text{year}$ and $v_{\infty} = 500 \text{ km/s}$, with $\beta = 2.0$, for the velocity profile. We obtained line force parameters that corresponds to a δ -slow solution, with the following wind parameters: $\dot{M} = 0.24 \times 10^{-6} M_{\odot}/\text{year}$ and $v_{\infty} = 254 \text{ km/s}$.

From Figure 4, we can observe the difference between the velocity profile (β -law) used by Haucke *et al.* (2018) and our hydrodynamic profile (δ -slow solution).

4. Conclusions

According to our experience in spectral line fittings, we predict that the models with values of $\beta \gtrsim 1.5$ can be properly reproduced with the hydrodynamic solution δ -slow. Currently, in our methodology, all the lines have the same weight, but we are testing to assign different weight to those lines that could have more impact on stellar parameters (e.g., silicon transitions in the effective temperature).

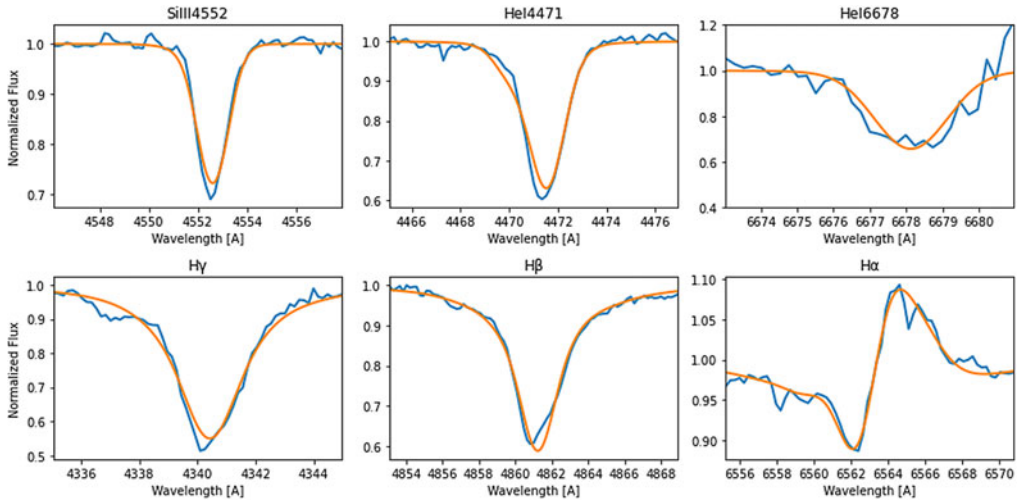


Figure 3. Spectral line fitting for HD 99953. Blue solid line shows the spectra retrieved from Haucke et al. (2018). Orange solid line corresponds to a model with the following parameters: $T_{\text{eff}} = 18500$ K, $\log g = 2.4$, $\alpha = 0.45$, $k = 0.15$, $\delta = 0.34$, $v_{\text{micro}} = 15$ km/s and $\log \epsilon_{\text{Si}} = 7.81$.

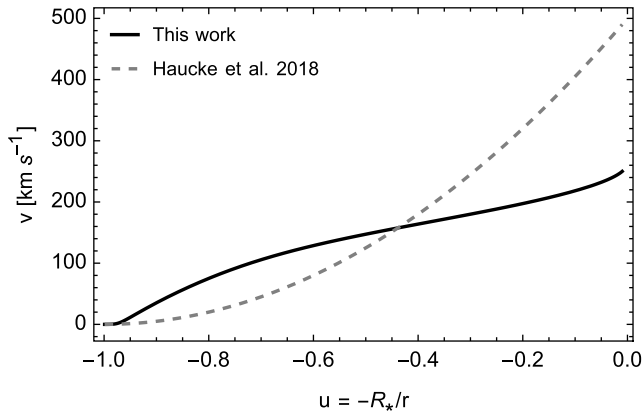


Figure 4. Comparison between the velocities profiles used to fit the spectral lines.

Further studies with more stars and analysis of more spectral lines will give us more precise estimates of the stellar and wind parameters, leading us to calibrate the WLR accurately.

As future work, we expect to analyze the χ^2 distributions and then use it to compute the uncertainties for each derived parameter, also, we are working in a statistical study of the theoretical line profiles shapes in contrast with stellar and wind parameters from ISOSCELES in order to study the influence of the wind in the observed line profiles.

Acknowledgements

M.C., C.A., & I.A. are grateful with the support from FONDECYT project 1190485. I.A. & C.A. also thanks the support from FONDECYT projects 11190147 and 11190945, respectively. This project receive funding from the European Union's Framework Programme for Research and Innovation Horizon 2020 (2014–2020) under the Marie Skłodowska-Curie grant Agreement No. 823734.

References

- Castor, J. I., Abbott, D. C., & Klein, R. I. 1975, *ApJ*, 195, 157
- Curé, M. 2004, *ApJ*, 614, 929
- Curé, M., Cidale, L., & Granada, A. 2011, *ApJ*, 737, 18
- Ekström et al., 2008, *A&A*, 489, 685
- Friend, D. B., & Abbott, D. C. 1986, *ApJ*, 311, 701
- Gormaz-Matamala, A. C., Curé, M., Cidale, L. S., & Venero, R. O. J. 2019, *ApJ*, 873, 131
- Haucke, M., Cidale, L. S., Venero, R. O. J., Curé, M., Kraus, M., Kanaan, S., & Arcos, C. 2018, *A&A*, 614, A91
- Puls, J., Springmann, U., & Lennon, M. 2000, *A&AS*, 141, 23
- Puls, J., Urbaneja, M. A., Venero, R., Repolust, T., Springmann, U., Jokuthy, A., & Mokiem, M. R. 2005, *A&A*, 435, 669
- Simón-Díaz, S., & Herrero, A. 2014, *A&A*, 562, A135